Accepted manuscript (Water Research): https://doi.org/10.1016/j.watres.2023.119740

Isotopically labeled ozone: a new approach to elucidate the formation of ozonation products

Millaray Sierra Olea[a], Simon Kölle[a], Emil Bein[a], Thorsten Reemtsma[b,c], Oliver J. Lechtenfeld[b,d], and Uwe Hübner[a]*

[a] Chair of Urban Water Systems Engineering, Technical University of Munich, Am Coulombwall 3, D-85748 Garching, Germany

[b] Department of Analytical Chemistry, Helmholtz Centre for Environmental Research – UFZ, Permoserstrasse 15, 04318 Leipzig, Germany

[c] Institute of Analytical Chemistry, University of Leipzig, Linnéstrasse 3, 04103 Leipzig, Germany

[d] ProVIS–Centre for Chemical Microscopy, Helmholtz Centre for Environmental Research–UFZ, Permoserstrasse 15, 04318 Leipzig, Germany

* Corresponding author: Chair of Urban Water Systems Engineering, Technical University of Munich, Am Coulombwall 3, D-85748 Garching, Germany

E-mail: u.huebner@tum.de (U. Hübner)

Abstract

As ozonation becomes a widespread treatment for removal of chemicals of emerging concern in wastewater treatment plant effluents, there are increasing concerns regarding the formation of ozonation products (OPs), and their possible impacts on the aquatic environment and eventually human health. In this study, a novel method was developed that utilizes heavy oxygen ($^{18}O_2$) for the production of heavy ozone ($[^{18}O_1]O_2$, $[^{18}O_2]O_1$, $[^{18}O_3]$) to actively label OPs from oxygen transfer reactions. To establish and validate this new approach, venlafaxine with a well-described oxygen transfer reaction (tertiary amine -> *N*-oxide) was chosen as a model compound. Observed $^{18}O/^{16}O$ ratios in the major OP venlafaxine *N*-oxide (NOV) correlated with expected ^{18}O purities based on tracer experiments. These results confirmed the successful labeling with heavy oxygen and furthermore demonstrate the potential to monitor NOV as an indicator of $^{18}O/^{16}O$ ratios during ozonation. As a next step, $^{18}O/^{16}O$ ratios were used to elucidate the formation mechanism of previously described OPs from sulfamethoxazole (SMX). Seven OPs were detected including the frequently described nitro-SMX, which was formed with a maximum yield of 3.2% (of initial SMX). With the successful labeling of six of the seven OPs from sulfamethoxazole, it was possible to confirm their previously proposed formation pathways, and distinguish oxygen transfer from electron transfer reactions.

$^{18}O/^{16}O$ ratios in OPs indicate that hydroxylation of the aromatic ring and formation of nitro-groups mostly follows oxygen transfer reactions, while electron transfer reactions initiate the formation of hydroxylamine and the abstraction of NH_2 leading to catechol.

Keywords: ozonation products, oxygen-18, isotope labeling, wastewater

1. Introduction

Chemicals of Emerging Concern (CECs) have their origin in our daily domestic and industrial applications (Loos et al., 2013; Margot et al., 2013). The main concern with CECs is related to their biologically active design and wide range of application (Lee and Von Gunten, 2016). Their high polarity and poor degradability (high persistence) prevents the efficient removal in conventional WWTPs (Reemtsma et al., 2006), which results in constant discharge into surface waters at detectable concentrations (ng L^{-1} to µg L^{-1}) (Margot et al., 2013; Ternes et al., 2003). Ozonation is an advanced treatment technology currently used in wastewater treatment plants (WWTPs) to reduce the concentrations of CECs in their discharged effluent (Bourgin et al., 2018; Eggen et al., 2014; Gulde et al., 2021; Huber et al., 2005; Margot et al., 2013; Ternes et al., 2003). Despite the known benefits of ozone for oxidation, which often leads to immediate loss of biological activity (e.g., hormones, antibiotics) (Huber et al., 2004) there are still uncertainties regarding the transformation of CECs into a mix of unknown and potentially hazardous ozonation products (OPs) (Hübner et al., 2015; Lee and Von Gunten, 2016; Wert et al., 2007).

OPs are formed by the partial oxidation of compounds when they react with ozone (von Gunten, 2003; Von Sonntag and Von Gunten, 2012). The selective reaction of ozone often results in a limited number of major OPs (Lim et al., 2019; Zucker et al., 2018), with their formation controlled by the reactive functional groups in the parent compound (Tentscher et al., 2019). In contrast, diffusion controlled reactions with hydroxyl radicals (•OH), that are generated as secondary oxidants from ozone reactions with the water matrix, form numerous OPs at low individual concentration (von Gunten, 2003).

With the current understanding of ozone reaction mechanisms, examples of OPs formation from parent functional groups, are: *N*-oxides and dealkylated products formed from tertiary amines, nitroalkanes and or hydroxylamines formed from aliphatic primary and secondary amines, hydroxylated compounds formed from aromatic scaffolds, as well as aldehydes and ketones formed from unsaturated carbons chains (Lee and Von Gunten, 2016; Lim et al., 2019; Tekle-Röttering et al., 2016; Zucker et al., 2018). Nevertheless, knowledge gaps still exist for ozonation reaction kinetics and mechanisms for Sulfur (S) and Nitrogen (N) containing moieties. In S- containing moieties (thiols, thioethers, and disulfides), the formation of a sulfoxide (SO) has been proposed as the most common functional group (Dodd et al., 2010), but only limited knowledge about the possible subsequent reactions to form sulfone (SO_2), sulfonic acid (SO_3H), and sulfate (SO_4^{2-}) is available (Lim et al., 2022). For *N*- containing moieties, there is uncertainty in the case of secondary amines, where, although hydroxylamines were suggested as a major product, studies have shown that this might be only an intermediate and nitro-alkanes are the major OPs (Lim et al., 2022).

In previous experiments focused on drinking water treatment, the use of isotopically labeled (^{13}C, ^{15}N and ^{2}H) parent compounds facilitated the identification of reaction sites for ozone, as well as, the elucidation of the formed OPs by their characteristic isotopic pattern (Brunner et al., 2019; Kolkman et al., 2015; Liu et al., 2019; Spahr et al., 2015; Spahr et al., 2017). The use of labeled compounds and stable isotope analysis (^{13}C, ^{14}C, ^{15}N and ^{2}H) has also been applied to study different CECs, to identify their OPs and elucidate their formation pathways in WWTP (Betsholtz et al., 2022; Borowska et al., 2016; Mawhinney et al., 2012; Willach et al., 2017). These studies have focused on particular compounds considered relevant, either by their abundance or by their toxicity, but were not based on the reactivity of the specific functional groups with ozone. Because of the overwhelming number of CECs and organic matter in wastewater, rather than evaluating every single compound and its OPs in a complex mixture, it is more efficient to generate transferable knowledge regarding individual functional group reactivity with ozone and the expected OPs (von Gunten, 2018).

The objective of this study is to establish and validate a novel isotope labeling method by using isotopically labeled ozone ($[^{18}O]_3$) to oxidize selected model compounds and produce isotopically labeled OPs. The method has been validated by the ozonation of a model substance (venlafaxine) with well-known reaction mechanism with ozone (tertiary amine -> *N*-oxide), and then applied to investigate the reaction mechanism of

sulfamethoxazole (sulfonamide) leading to formation of 4-nitro-sulfamethoxazole and other OPs. By using this approach, we put emphasis on functional group reactivity towards ozone. This alternative approach can provide information such as reaction site/preference when more than one functional group is present, explicit reaction mechanism and reaction pathway for OPs formation, and enable the detection of OPs formed during ozonation of complex wastewater or drinking water matrices. In a parallel study, we successfully implemented this new concept for the detection of products during the ozonation of effluent organic matter (EfOM) (Jennings et al., 2022).

2. Materials and Methods

2.1. Chemicals and reagents

For sample preparation, the following compounds were used: venlafaxine hydrochloride (VLX), sulfamethoxazole (SMX), primidone (PRI), and tert-butanol (t-BuOH, ≥99 %). Technical O_2 and N_2 gases were used for initial testing of the system. Heavy oxygen gas ($^{18}O_2$ ≥97%) was used for the production of labeled ozone. Additional information regarding the chemicals and gases used can be found in the SI, Table S 1.

2.2. Generation of labeled ozone stock solution

Configuration of the ozonation system. A previously established ozonation system (Müller et al., 2019) was modified with the addition of two gas feedlines ($^{18}O_2$, N_2) and the positioning of 2- and 3-way valves (SI, Figure S 1). These modifications allow the system to be operated as a closed-circuit with the possibility of recovering the used $^{18}O_2$ from the experiments. In closed-circuit operation, the system had an approximate gas volume of 600 mL. A bellows pump (5 NL min^{-1}) was used to maintain and guarantee the gas flow inside the system. For gas conditioning, two water traps with molecular sieve 3 Å were placed before the ozone generator. The reactor volume was 500 mL and a needle valve port was implemented for the controlled extraction of the ozone stock solution. For additional information regarding the operation of the system and its components, refer to SI Text S 1 and Table S 2.

Generation of the ozone solution. The operational procedure to generate the stock solution with labeled ozone followed five steps including: i) initial feeding with technical O_2 gas, ii) changing to $^{18}O_2$ (≥ 97%) as input gas until desired $^{18}O/^{16}O$ ratios were reached, iii) switching to closed-circuit operation, iv) ozone generation, stock solution generation and ozonation batch experiments, and v) switching to open-circuit operation with recovery of $^{18}O_2$. In phase iv, ozone was generated using a BMT 803 BT ozone generator and continuously bubbled into the reactor, which was filled with ultrapure water and cooled in an ice-filled container (~4°C). Required volumes of ozone stock solution (to set a concentration of approximately 25 mg L^{-1}) were extracted from the reactor using a gastight glass syringe. This volume was used to determine the dissolved ozone concentration in the stock solution and for the ozonation of the samples. The dissolved ozone concentration was measured by the colorimetric indigo carmine method (Bader and Hoigné, 1981).

Determination of mixing ratios using N_2 and O_2 gases. Because the change from $^{16}O_2$ to $^{18}O_2$ could not be monitored, tracer tests with N_2 and O_2 gases were conducted to determine optimum times for operation (opening and closing) of the gas lines, as well as establishing the optimal conditions of gas pressure and flow. The test was performed by initially saturating the system with 100% O_2 gas until stable reading in an inline oxygen sensor (FTC-SU-PSt3, Presens Precision Sensing GmbH, Germany). Subsequently, the two valves controlling O_2 and N_2 were simultaneously closed and opened, respectively. Finally, after a pre-determined amount of time, the valve controlling the system mode (open circuit vs. gas recirculation) was closed. The breakthrough curves obtained from the shift from 100 % O_2 to N_2 as well as the final mixing ratios were monitored in the inline oxygen sensor. The expected losses of ^{18}O gas were calculated by integrating the measured oxygen concentration over time during open-circuit feeding of the system and recovery after the experiment.

2.3. Batch ozonation experiments

Sample preparation. Samples for batch experiments with VLX and VLX/SMX were prepared in separate 20 mL vials. To elucidate the reaction mechanism of ozone with model compounds, the formed hydroxyl radicals (•OH) were scavenged by using t-BuOH with a $k_{OH} = 6 \times 10^8\ M^{-1}\ s^{-1}$ (Von Sonntag and Von Gunten, 2012). The concentrations of t-BuOH were adjusted to the compound concentration in experiments with VLX and VLX/SMX as described in SI, Text S 2. In addition,

primidone with a k_{O3} = 1 M^{-1} s^{-1} and k_{OH} = 6.7 x 10^9 M^{-1} s^{-1} (Real et al., 2009) was used as a radical indicator. Removal of primidone <5 % confirmed efficient radical scavenging by t-BuOH in all experiments. In parallel, samples without t-BuOH were prepared. All samples for ozonation were prepared in phosphate buffer at pH 7. A detailed composition for each batch experiment is provided in SI, Table S 3.

Ozonation experiments. To establish the labeling method and validate its performance, initial experiments with VLX as sole ozone reactive compound were performed. As reported by Zucker et al. (2018), the major ozonation product of venlafaxine is venlafaxine-*N*-oxide (NOV). The reaction mechanism of this compound proceeds by the transfer of one oxygen atom from the ozone molecule to the nitrogen of the tertiary amine functional group (SI, Figure S 3). Alternative transformation reactions (i.e., *N*-dealkylation, ozone attack at the activated aromatic ring) were not considered since they were only expected to affect the yield of NOV but not its $^{18}O/^{16}O$ ratio.

Consequently, a total of six experiments was performed. Four experiments were completed with VLX as sole target compound, one experiment: with technical ^{16}O gas, and three experiments with different targeted $^{18}O/^{16}O$ ratios (adjusted with different gas loading times). In these batch experiments 20 µmol L^{-1} of VLX was oxidized using ozone dosages of 10 - 100 µmol L^{-1}. The approach of labeling of OPs with ^{18}O was then applied to investigate transformation reactions for SMX with two different $^{18}O/^{16}O$ ratios. A molar ratio of 1:5 for VLX/SMX (10 µmol L^{-1} VLX, and 50 µmol L^{-1} SMX) was determined in preliminary tests to generate detectable peaks of OPs from both compounds. Samples were oxidized with ozone dosages of 50 - 300 µmol L^{-1}. A list of the targeted molar ratios for both compounds can be found in SI, Table S 4. The volume in all experiments was adjusted to 10 mL and samples were stored at 4°C until measurement.

2.4. Sample analysis

Compound quantification. Samples were measured on an LC-MS/MS (PLATINblue UHPLC – Knauer, Germany, ABSciex TQUAD 6500 – SCIEX, USA), using a method established and described by Müller et al. (2017). Quantification of VLX, venlafaxine *N*-oxide (NOV), SMX and PRI was accomplished in positive MRM (multiple reaction monitoring) mode. The quantification of the OP 4-nitro sulfamethoxazole (NIT), was performed in negative MRM mode. To determine the $^{18}O/^{16}O$ ratio in labeled NOV and

NIT, the qualifying and quantifying fragments´ *m/z* values were modified to include the expected labeling site and mass shift. For additional information regarding Q1 (precursor ion) and Q3 (product/fragment ion) masses and internal standards, refer to SI, Table S 5.

Separation and detection of SMX OPs. The separation of the OPs from SMX was performed with a Waters XSelect HSS T3 column (100Å, 3.5 µm, 2.1 mm x 100 mm, Waters Germany) on an LC-MS system (Agilent 1260 Infinity – Agilent Technologies, USA, ABSciex Qtrap 5500 - SCIEX, USA). For the separation of the compounds, a gradient method was developed (SI, Table S 6). The solvents used were, ultrapure water (Arium Pro, Sartorius AG, Göttingen, Germany) and acetonitrile (hypergrade for LC-MS, LiChrosolv, Merck KGaA, Darmstadt, Germany) supplemented with 0.1 % formic acid (LC-MS grade, HiPerSolv, VWR Chemicals, Leuven, Belgium). For compound detection in negative mode, Enhanced MS Scan (EMS) and Enhanced Product Ion Scan (EPI) were applied. The mass ranges used in both scan types can be found in SI, Table S 7. Data exploration and integration of the peak areas was performed with the software Analyst 1.6.2 (ABSciex - SCIEX, USA).

2.5. Data handling and calculations

Analysis of SMX OPs. For the integration of peak areas of the labeled SMX OPs, isotopologue fractions (IF) for the monoisotopic mass and the integration of up to two labeled oxygen atoms were determined according to Mairinger and Hann (2020). Data was acquired in profile mode for both MS experiments, with a step size of 0.12 Da for a series of evenly spaced discrete mass values. The MS^1 mass spectra of individual samples and their isotopologue peaks were analyzed focusing on their centroid mass (Da), peak start (Da) and peak end (Da). Mean and standard deviation of discrete *m/z* ranges were used to define the starting and ending values for the different isotopic distribution of the isotopologues (SI, Table S 8). Once discrete and nonoverlapping *m/z* ranges were determined, isotopologue peak areas with M+0 ([^{16}O]), M+2 Da ([^{18}O]) and M+4 Da (2 [^{18}O]) were integrated (SI, Table S 9). It should be noted that these calculations were performed by evaluating MS^1 data with low resolution.

Oxygen transfer reaction probabilities. The $^{18}O/^{16}O$ ratios determined in the formed NOV (from single oxygen transfer reaction to VLX) were applied to elucidate the formation pathway of OPs from SMX. These $^{18}O/^{16}O$ ratios were used to calculate the expected isotopologue fractions during the formation of SMX OPs with two oxygen

additions (eq. 1), where *x* and *y* denote the number of ^{16}O and ^{18}O atoms and Pr(^{16}O) and Pr(^{18}O) represent the probabilities determined by VLX measurements (modified from Valkenborg et al. (2012)).

$$Pr\left(^{16}O_x\ ^{18}O_y\right) = \frac{(x+y)!}{x! \times y!} \Pr\left(^{16}O\right)^x \times \Pr\left(^{18}O\right)^y \quad (1)$$

However, this calculated isotopologue distribution does not yet consider the natural isotopologues of the parent molecule. The web platform *enviPat* (Loos et al., 2015) was used to predict the expected isotopic pattern of SMX + 2O, and the relative abundance of relevant natural isotopologues (monoisotopic mass [M], M+2) (SI, Text S 3). As an example, the calculated distribution of SMX-OPs with and without consideration of natural isotopologues are illustrated in SI, Figure S 4 for assumed probabilities of ^{18}O (Pr(^{18}O)) of 0%, 30% and 90%. Results indicate a limited effect of the natural isotopologues on the distribution of ^{18}O-OPs from SMX, but this might become different for ozonation of larger molecules, especially if they contain several atoms with naturally abundant stable isotopes of +2 Da (e.g., sulfur). These hypothetical values were then contrasted with the empirical results obtained from signal intensities of SMX OPs.

3. Results and Discussion

3.1. Method development and validation

The establishment and validation of the novel labeling method was performed as follows: (1) evaluation of N_2 and O_2 gas mixing ratios, (2) quantification of the $^{18}O/^{16}O$ ratio in NOV, and (3) correlation of the gas mixing ratios with labeling success of NOV. Following this approach, we were able to confirm the suitability of VLX to indicate the $^{18}O/^{16}O$ of OPs from oxygen transfer reactions.

Determination of mixing ratios using N_2 and O_2 gases. The percentage of $^{18}O_2$ depends on the gas loading time (seconds), which is the duration of gas feeding from the $^{18}O_2$ container before the ozonation system is changed to recirculation mode. We simulated $^{18}O_2$ percentage by exchanging O_2 with N_2. Initially, nine different gas loading times were tested during operation at 0.5 bar generator pressure in replicate experiments (minimum 2 to up to 17 replicates for most promising settings) and gas loading times were compared with regards to their mixing ratios (simulated percentage of $^{18}O_2$)

(Figure 1A). In addition, the volume of gas that could not be recovered for future experiments (Figure 1A) was determined (gas loss). Since an increase in gas loading times beyond 17 s did not considerably improve the gas percentage to values > 90 %, this operational setting was selected for experiments with the highest percentage of labeled ozone production (91.4 %). In addition, experiments with 9 s were conducted to obtain the lowest percentage of $^{18}O_2$.

After slight modifications of the ozone system (increased volume from additional dehumidification, higher generator pressure of 0.9 bar), experiments were repeated with slightly different gas loading times of 13 s and 21 s. Two example breakthrough curves are shown in Figure 1B. Results demonstrate that full breakthrough is reached after approximately 30 - 40 s, followed by several minutes of oscillation in the recirculated system until both gases are fully mixed. In addition, the black arrow in Figure 1B demonstrates the impact of pressure on the oxygen sensor, as the 20 % increase in O_2 gas can only be explained by a pressure change in the system after switching from gas feeding to recirculation (see SI, Text S 4 for details). Finally, the type of gas being exchanged (O_2 to N_2 vs N_2 to O_2) seems to affect the results (SI, Figure S 5).

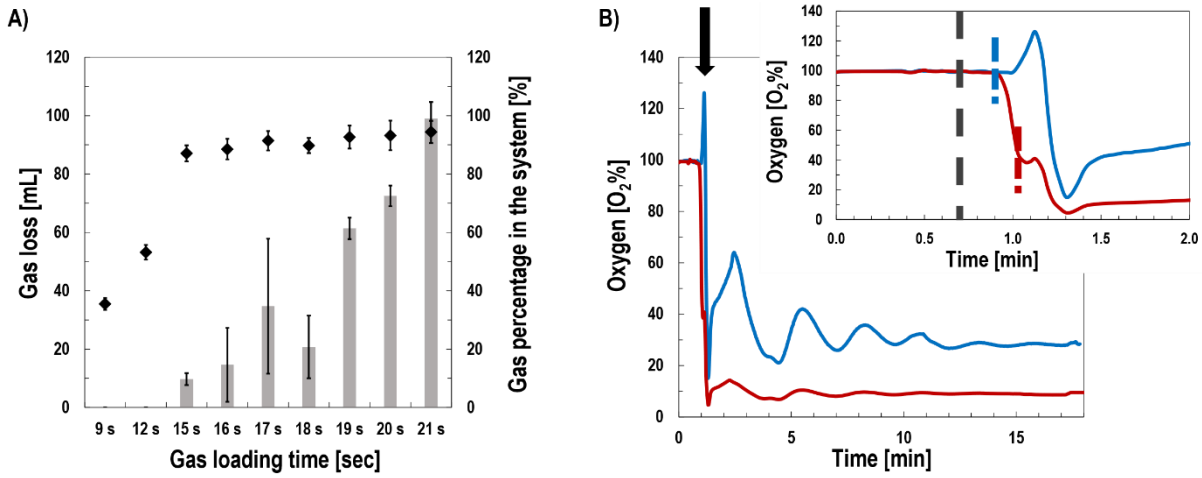

Figure 1. (**A**) The percentage of $^{18}O_2$ that is expected depending on the gas loading times (diamonds), as well as, the volume of gas that would be lost in each of the tested times (bars). Error bars indicate standard deviation from variable number of replicates (2 - 27) at different times. (**B**) Change of O_2 concentration in the system during tests with O_2 and N_2. The inlet shows the first 2 min with the dotted black line indicating the change of gas lines, the dotted blue and red lines the times the system was closed.

Determination of $^{18}O/^{16}O$ ratios using NOV. With the operational protocol established, the expected ^{18}O gas percentage simulated with the tracer N_2/O_2 experiments were

corroborated by performing heavy ozone experiments and using the ozonation product NOV of VLX as indicator of labeling success. As a reference for the isotope distribution of OP formed by ozonation, the relative ion intensity of NOV in an experiment with $^{16}O_3$ was quantified (97 % *m/z* 294 $[M+H]^+$ and 3 % *m/z* 296 $[M+H]^+$). This isotope pattern was additionally compared with the values obtained from the calculation performed by using the *enviPat* platform (Loos et al., 2015) (SI, Text S 5). Because these samples were analyzed with an MRM method, with modified Q1 and Q3 masses that considered the labeled fragment, other possible isotopologues were not measured.

In Figure 2A, the percentage of labeled NOV in ozonation experiments with different $^{18}O/^{16}O$ ratios is shown as a function of the transformed VLX at different ozone dosages. The oxygen transfer reaction was confirmed by the changes in the relative abundance of the isotopic fraction of the detected peaks ([M+0], [M+2]) of the produced NOV. Therefore, when comparing the values for *m/z* 294 $[M+H]^+$ and *m/z* 296 $[M+H]^+$ obtained in the $^{16}O_3$ experiments, with the results observed in the produced NOV *m/z* of the different $^{18}O/^{16}O$ ozone experiments, the labeling efficiency was reflected in the results, where the highest labeling efficiency was 79 ± 1% ^{18}O-NOV, meanwhile the lowest was 43.9 ± 0.3% ^{18}O-NOV. The results of these experiments show that the $^{18}O/^{16}O$ ratios of the labeled NOV are stable and independent of the removed VLX, and ozone concentration dosed.

Additionally, as shown in Figure 2B, the $^{18}O/^{16}O$ ratio of labeled NOV changed according to the simulated concentrations of $^{18}O_2$ (O_2/N_2 ratio) in the system. Increasing the proportion of heavy oxygen in the ozonation system, increased the proportion of the heavy-labeled transformation product (^{18}O-NOV). The correlation between both variables was found to be $R^2 = 0.9605$, which indicates that ^{18}O-NOV formation is a suitable proxy for the estimation of the $^{18}O/^{16}O$ ratio.

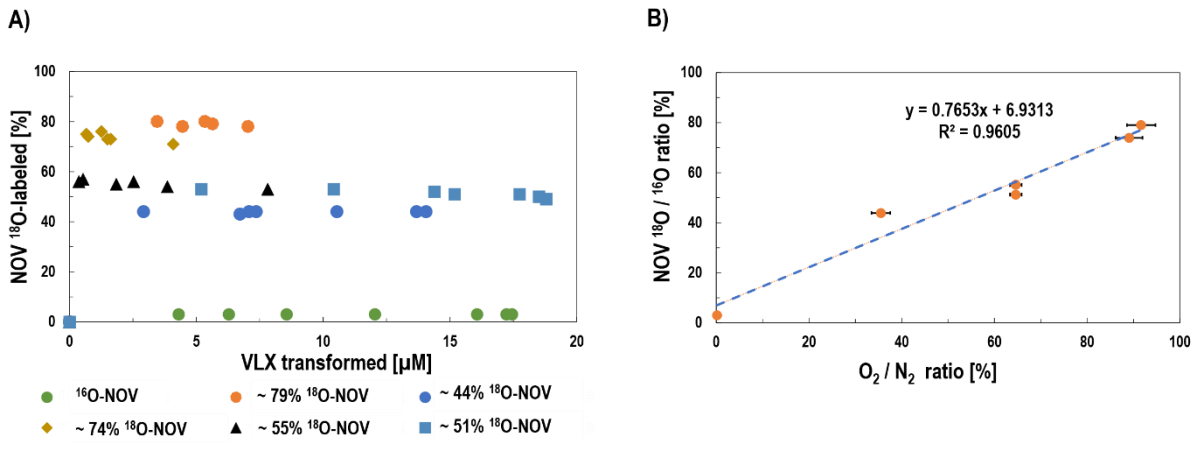

Figure 2. (**A**) Labeling efficiency of NOV depending on the ^{18}O /^{16}O ratios applied in the ozonation experiments with different $^{18}O_3$ concentrations (**B**) the relative intensity of the labeled NOV for the experiments with a range of different $^{18}O_3$ / $^{16}O_3$ concentrations compared to expected ratios from N_2/O_2 experiments ($y = 0.7653x + 6.9313$, $R^2 = 0.9605$).

However, as can be seen in Figure 2B the labeling success has an observable scattering that can be explained by different factors. First, the system is operated manually and the changing of the gas lines must be done in seconds, thus any millisecond delay or mistake will considerably impact the gas percentage. Second, the estimation of the oxygen percentage depends on the pressure in the gas line (see change of O_2 % in Figure 1B due to switching from open to closed-circuit), therefore a higher reading of the oxygen sensor has an impact on the results obtained in the gas mixing experiments (O_2/N_2 ratios) (SI, Figure S 6). Third, two different purities of $^{18}O_2$ were used for the production of ozone, the first had a purity of 99 ^{18}O % (Sigma-Aldrich, USA), the second 97 ^{18}O % (Linde GmbH, Germany). Fourth, the kinetic isotope effect is not expected since VLX is present in excess and all the ozone is consumed. Under these conditions, there is no distinction between the heavy and the light ozone. In conclusion, the isotopic pattern of the formed NOV can be used as a surrogate to establish $^{18}O/^{16}O$ ratios for experiments with other compounds and matrices.

3.2. Pathways for the reactions of sulfamethoxazole with ozone

Quantification and semi-quantification of SMX OPs. In experiments with ^{16}O-ozone, six OPs were detected (SI, Figure S 7). These products were previously reported in other studies, providing MS data and possible formation pathways (Gao et al., 2014; Gómez-Ramos et al., 2011; Willach et al., 2017). Additionally, it was possible to detect a seventh previously unreported OP, OP284. To confirm the chemical identity of OP282a, the commercially available standard for 4-nitro-sulfamethoxazole (NIT) was used, which also enabled its quantification (SI, Figure S 8). The yield of NIT was 3.2 ± 0.3 % based on the complete abatement of SMX (SI, Figure S 9). The isotopologue distributions can be analyzed to distinguish OPs formed by oxygen transfer from ozone from other types of reactions. While OPs with $^{18}O/^{16}O$ ratios measured in NOV are derived from oxygen transfer by ozone, OPs with unlabeled oxygen may derive from other sources, e.g. through hydrolysis. Also transfer reactions from dissolved oxygen would generate lower $^{18}O/^{16}O$ ratios as a result from mixing the ozone stock solution (oversaturated with the applied $^{18}O/^{16}O$ ratio) with the sample

containing ambient dissolved oxygen without the label. The resulting ratios would also change with increasing ozone dosage. Additionally, there was no significant difference in the removal of SMX and the formation of labeled NIT, regardless of the $^{18}O/^{16}O$ ratio used for the production of the labeled ozone.

Peak areas of the seven OPs can be found in SI, Figure S 10. There, the formation of the OPs is illustrated as a function of the SMX removal. The comparison of cumulative intensities from isotopologues (IF) with results from ozonation with technical oxygen does not show any systematic deviation that would indicate different behavior of ozonation with different $^{18}O_2$ abundances.

Application of $^{18}O/^{16}O$ ratios in VLX/SMX ozonation. Figure 3 illustrates measured isotopologue distributions for all detected SMX-OPs in comparison to the expected distribution for transfer of one oxygen (indicated by NOV distribution) and the expected probabilities for two oxygen transfer reactions (shown as 2O transfer).

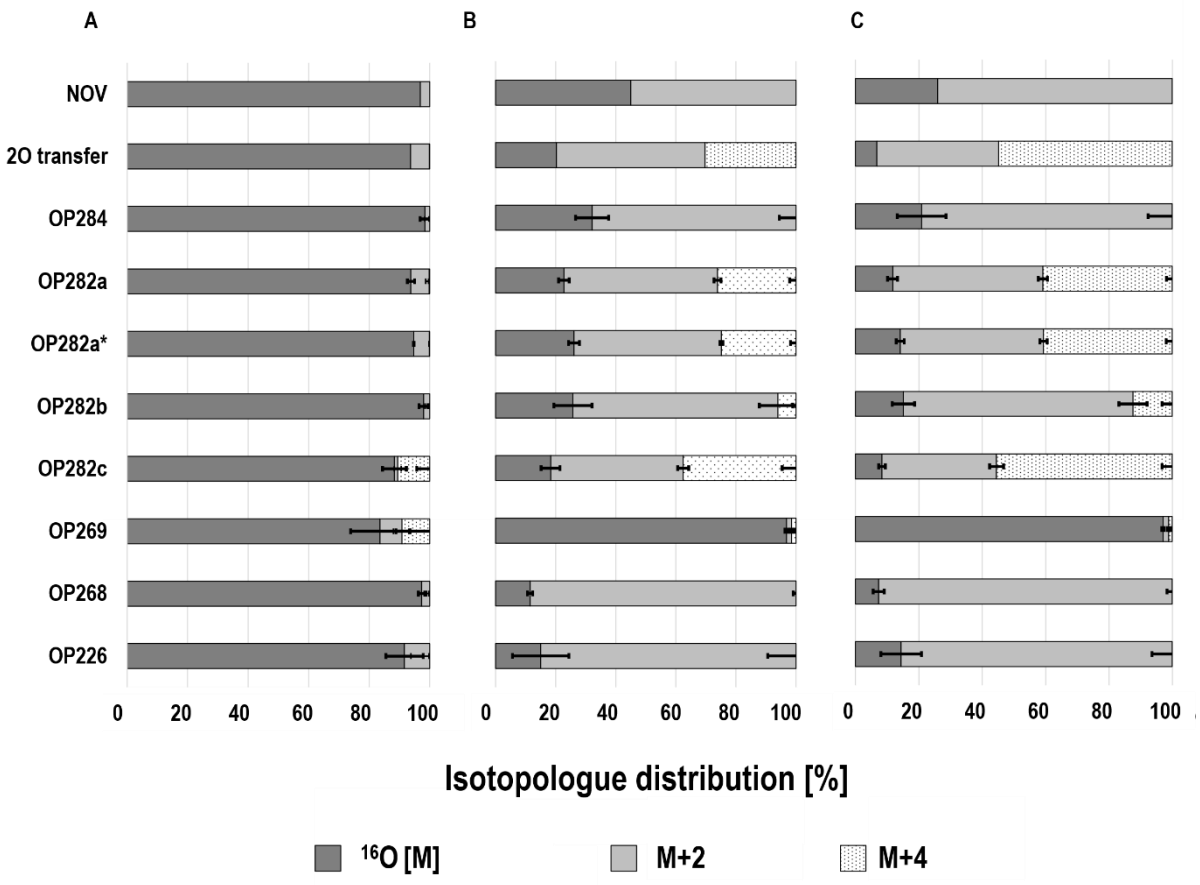

Figure 3. Change of the isotopologue distribution in the formation of different SMX OPs. OPs obtained from ozonation (**A**) with technical oxygen are compared to OPs obtained from ozonation (**B**) with a 55 ± 1.5 % ^{18}O percentage, (**C**) and 74 ± 1.3 % ^{18}O percentage based on NOV measurements (OP282a* was quantified by MRM using

the transitions *m/z* 282/186, *m/z* 284/188 and *m/z* 286/190, while all other isotopologue distributions were derived from the intensity of the respective molecular ions). Error bars indicate standard deviation observed in the formation of labeled OPs being produced by different ozone dosages. Venlafaxine *N*-oxide (NOV) was used as an internal indicator of the $^{18}O/^{16}O$ ratio.

Six of the seven detected OPs from SMX showed a shift in their isotopologue fraction, showing similar isotopologue distribution as the measured NOV $^{18}O/^{16}O$ ratio. These shifts in the isotopic pattern of the ion indicate the successful addition of one or two ^{18}O atoms during ozonation. As can be seen by comparing isotopologue distributions in Figure 3, the three isomers of *m/z* 282 (NIT: OP282a, OP282b and OP282c) seemed to be a result of two oxygen transfer reactions from the labeled ozone. Isotopologue distributions of NIT were determined from integration of qualitative MS^1 data (shown as OP282a) and from MRM quantification (OP282a*). Overall, results show a good agreement between both analytical methods, indicating that MS^1 data is suitable to assess isotopologue distribution for other OPs without an available standard. Minor differences, although significant ($p\text{-value} < 0.05$) when comparing between the measurements of the isotopologues fractions of NIT (*m/z* 282, 284 and 286) and the results obtained from the integration of the fragments of interest in (OP282NIT*) (*m/z* 282/186, *m/z* 284/188 and *m/z* 286/190 of the 55 % $^{18}O_2$), can be explained by the higher selectivity of the MRM method and the different criteria used for the data integration. OPs 282b and 282c showed stronger deviation from expected distribution for 2O transfer reactions. The *m/z* 286 isotopologue of OP282c (+4 Da) after ozonation with $^{16}O_3$ was higher than expected from natural abundances. However, this peak might also come from a different molecule that elutes at the same retention time, which can explain the shift in all experiments. In contrast, limited formation of *m/z* 286 for OP282b might be related to reactions with dissolved oxygen, which contains lower $^{18}O/^{16}O$ ratios after mixing of the sample with the stock solution.

The formation of OP284, OP268, and OP226 can be explained by one oxygen transfer reaction (Figure 3). The observed deviation in their ^{18}O content from the value expected from NOV may be due to their low peak areas. While OP268 and OP226 are solely generated through oxygen transfer reaction, OP284 contains an additional oxygen, which was not derived from ozone. Lastly, OP269 is the single OP not being formed by a direct oxygen transfer reaction from the labeled ozone despite the addition of 2 oxygen atoms during the reaction (see the mechanistic discussion below). The direct reaction of O_3 with the aromatic ring or nitrogen functional group has been

proposed as formation pathway for several of the reported OPs of SMX (Gao et al., 2014; Gómez-Ramos et al., 2011; Willach et al., 2017). However, the ^{18}O-labeling approach developed in this study is the first to suggest the origin of the oxygen in the ozonation products. This illustrates how ^{18}O-labeling gives additional insight into the mechanism and transformation pathways during ozonation.

Elucidation of ozone reaction pathways. For the formation of NIT, two different formation pathways were proposed by Willach et al. (2017). Pathway A (reactions (1)-(3)) in Figure 4 was proposed based on the reaction of ozone as an H-abstractor with the formation of a radical pair, a subsequent cage reaction and release of water (Tekle-Röttering et al., 2016). Pathway B (reactions (4)-(6)) was proposed based on the insertion reaction of ozone at the nitrogen, where the intermediate would release a hydroperoxyl radical and form a nitroxyl radical, which would decay assisted by water once again forming sulfamethoxazole and NIT (Von Sonntag and Von Gunten, 2012). A third alternative, formation pathway C, was proposed by Yu et al. (2017) using density functional theory (DFT). They proposed a hydrogen atom transfer (HAT) mechanism as the first step, producing an amino radical and a •OOOH radical, which would recombine with the amino radical. This newly formed intermediate could have its H_2O_2 replaced by ozone, releasing O_2 and forming the nitro group (reaction (7)-(12)). These three previously proposed pathways have in common that the two transferred oxygen atoms originate from the ozone molecule. This agrees with the results obtained from the labeling experiments, where both transferred oxygen atoms are labeled according to the expected $^{18}O/^{16}O$ ratios. Therefore, it is not possible to distinguish based on probabilities, which one of these three pathways (Figure 4) is responsible for the formation of the nitro group.

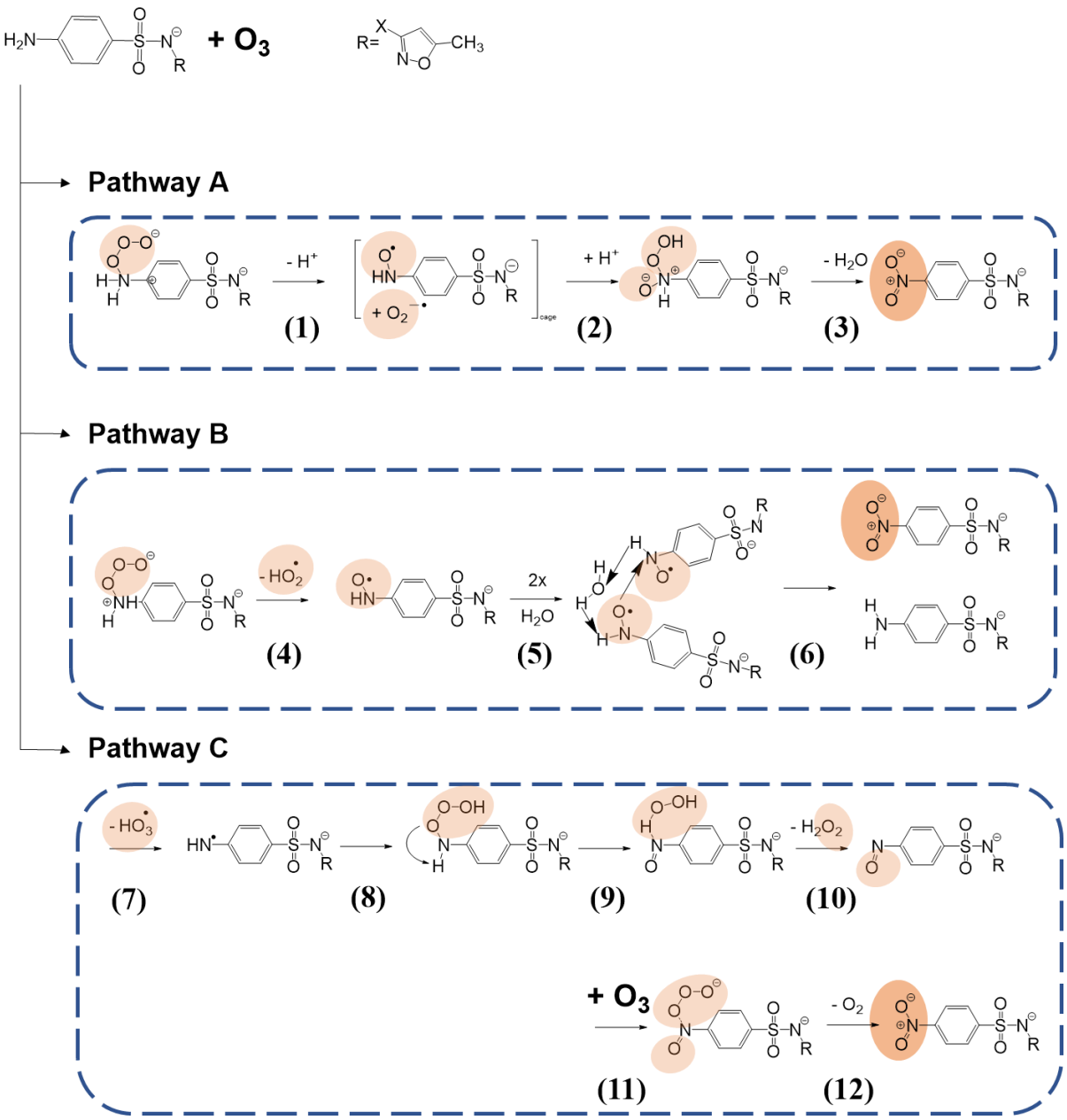

Figure 4. Three proposed formation pathway for the formation of 4-nitro-sulfamethoxazole (after Willach et al. (2017) and Yu et al. (2017)). Orange circles highlight the location of ^{18}O in presence of heavy ozone [$^{18}O_3$].

^{18}O labels in the proposed hydroxylated structures OP282b/c and OP268 indicate that hydroxylation predominately follows an oxygen transfer (addition) reaction as described by Tekle-Röttering et al. (2016) for aniline. In the case of OP268, a single hydroxylated OP, it was not possible to separate the two isomers described by Willach et al. (2017). In their study, they confirmed that one of these isomers was sulfamethoxazole hydroxylamine (OP268b), which can imply that the other detected isomer of OP268 (OP268a) could be formed by an oxygen transfer reaction from ozone to the aromatic ring (SI, Figure S 11, pathway D). For OP268b, they proposed an initial

H-abstraction from the anilinic nitrogen followed by a reaction with oxygen to form a peroxyl radical (Yu et al., 2017). Two peroxyl radicals would then decay to finally form the hydroxylamine (SI, Figure S 11, pathway E). In this formation pathway the transferred oxygen atom has its origin in the reaction of the aminyl radical with an oxygen molecule, which is contradicted by the observed shift in the isotope pattern of the formed OP268 (see Figure 3). Therefore, the formation pathway for the detected OP268a is better described by the transfer of an oxygen atom from the ozone molecule (Figure 5), although the precise location of the labeled oxygen could not be distinguished between the aromatic ring or the nitrogen moiety.

Gómez-Ramos et al. (2011) previously proposed the structure of OP282 b/c in Figure 5 based on HRMS measurements and the fragmentation pattern observed, which agrees with the results obtained in our work. For the formation of OP282 b/c (Figure 5) two oxidation equivalents were considered to propose a possible formation pathway. Here the initiation of the reaction could start as the suggested pathway D for the formation of OP268a (SI, Figure S 11), with an oxygen transfer at the aromatic ring. This would be followed by a second ozone attack at the nitrogen moiety, according to pathway C (reactions (7)-(10)), terminating after formation of the nitroso-group (SI, Figure S 12). An alternative formation pathway which considered first the formation of a nitrosobenzene via direct oxygen transfer to the aniline and a second ozone attack in the aromatic ring was not considered, because the nitrosobenzene moiety would be deactivated, therefore no secondary ozone reaction could take place. Other reasons for suggesting the aromatic ring as one of the reaction sites for ozone are the observed retention times for OP282 b/c (OP282b R_t: 6.7 min, OP282c R_t: 7.1 min) and their fragmentation patterns (SI, Figure S 14, Figure S 15). Furthermore, these two isomers are clearly not related to NIT, due to their significantly shorter retention times (NIT R_t: 17.2 min).

According to the MS^2 pattern observed for OP284 (SI, Figure S 16), this compound is formed by the addition of two oxygen atoms to the aniline ring structure (Figure 5). Its proposed structure presents hydroxylation at the nitrogen and the aromatic ring, but as mentioned above, only one of the two oxygens is labeled. Based on this observation, we propose that the labeled oxygen comes from the direct addition of ozone to the aromatic ring of the aniline (pathway D), while the second oxygen originates from a different reaction pathway. An electron transfer reaction at the nitrogen moiety was

proposed to generate a hydroxylamine (SI, Figure S 12, pathway E), but this reaction would also not explain the absence of a second label, because the transferred oxygen in the reaction should be partially labeled, too. As mentioned in the previous section, the production of this OP was limited and some uncertainty remains regarding the possibility of both oxygen atoms having their origin in direct oxygen transfers from the ozone molecule.

The suggested reactions are summarized as a proposed pathway for the transformation of SMX in Figure 5. Some of the intermediates expected after the first ozone attack (nitroso sulfamethoxazole and sulfamethoxazole hydroxylamine) were not detected in this study, but the SMX hydroxylamine was reported previously (Willach et al., 2017). Nonetheless, the formation pathway proposed in Figure 5 agrees with those previously established by Von Sonntag and Von Gunten (2012); Willach et al. (2017).

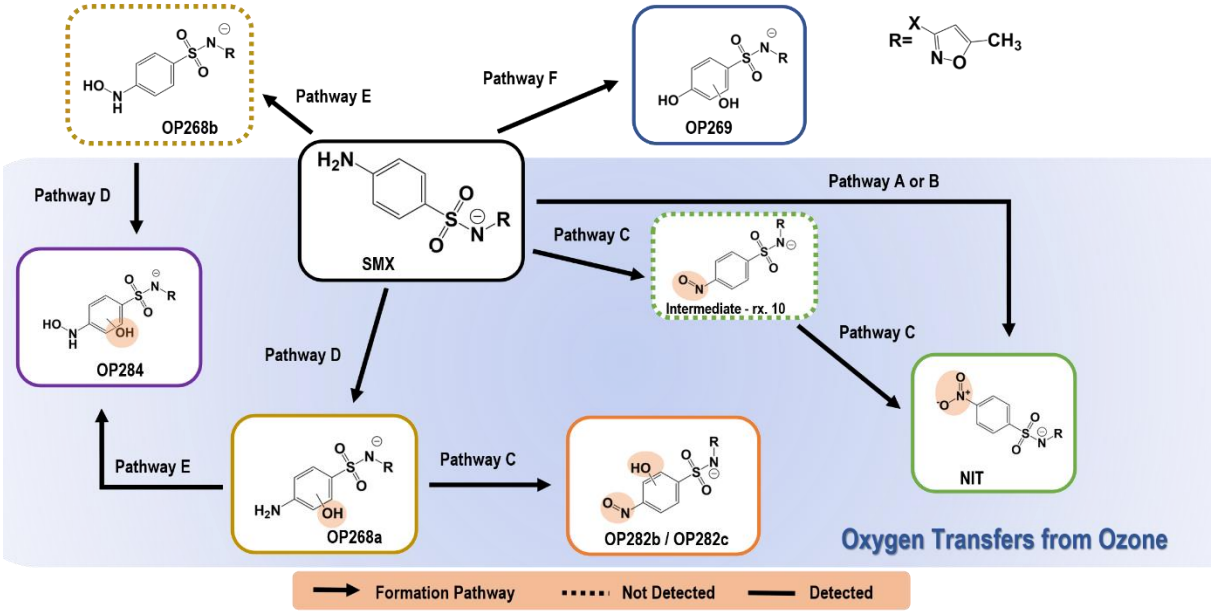

Figure 5. Overview of the formation pathways involved in the formation of six of the OPs of SMX. Detailed individual pathways are illustrated in Figures 4, S11, S12 and S13. Orange circles highlight the presence of ^{18}O.

For the formation of OP269, we can exclude a two-step reaction involving the hydroxylation of the aromatic ring by an oxygen transfer reaction, due to the lack of ^{18}O-labeling observed in the formed OP (see Figure 3). Furthermore, our results agree with the formation pathway proposed by Willach et al. (2017) for OP269, who hypothesized that the formation pathway is initiated by an ozone reaction at the aromatic ring, resulting in an electron transfer reaction (SI, Figure S 13, pathway F).

The ensuing reactions result in the cleavage of the anilinic nitrogen from the aromatic ring and its replacement by a quinone group (Willach et al., 2017).

Only one form of OP226 could be detected in the different ozonation experiments, unlike the two isomers reported by (Willach et al., 2017). Therefore, it can be concluded that the OP226 detected is not being produced by the reaction of SMX with a hydroxyl radical because of the presence of a radical scavenger. Furthermore, it can be stated with some certainty that the formation pathway involves the transfer of one oxygen atom from ozone.

Overall, the successful labeling of six of the seven detected SMX OPs confirmed the applicability of the new method to track the formation of ozonation products from compounds with aniline moieties. Furthermore, the $^{18}O/^{16}O$ ratio provided by the labeling of NOV was paramount to understand the origin of the transferred oxygen atoms and thereby supported the differentiation of previously proposed transformation pathways from oxygen transfer or electron transfer reactions.

4. Conclusions

This study presents a novel oxygen labeling technique with the aim to better understand ozonation reactions by elucidating formation pathways of OPs and discerning similarities in their formation based on the functional group available for ozone attack. Specifically, it was demonstrated that OPs being formed from oxygen transfer reactions from ozone have a distinct isotope pattern distribution, which distinguishes them from compounds formed by hydrolysis, hydroxyl radical reactions, or molecular oxygen. The major conclusions are:

- The formation of labeled venlafaxine *N*-oxide (+2 Da) confirmed the transfer of one ^{18}O atom to the tertiary amine of the model compound. The ratio of $^{18}O/^{16}O$ in the formed venlafaxine *N*-oxide correlated with determined gas ratios in previous tracer tests with N_2 and O_2 at the same operational settings. Therefore, venlafaxine *N*-oxide can be used as an indicator of ^{18}O percentage in the system. The measured $^{18}O/^{16}O$ ratios obtained from NOV formation can be used to confirm the origin of the transferred oxygens in newly formed OPs.
- The results corroborate that the labeling technique can be used to study the reaction mechanism of ozone, when a transfer of oxygen is involved. At the same time, it is

necessary to assess the possible reactions of $^{18}O_2$ with other radical species and how this can impact the formation of transformation products. Consequently, we propose the use of $^{18}O_3$ as a suitable tool to investigate the reaction of ozone with organic chemicals in a wide range of scenarios.

- Besides the observed suitability for the elucidation of formation mechanisms and pathways, the integration of this new labeling method will enable the detection of OPs from chemicals with multiple reactive sites and in complex water matrices. In a parallel study this approach has already been applied to identify products formed when effluent organic matter from secondary effluent is ozonated (Jennings et al., 2022).
- An additional potential application of this labeling method is the tracking of OPs and their characteristic newly formed functional groups in biological post-treatment to better understand their stability and persistence in the environment. The presence of the labeled functional group can be used to assess the generation of recalcitrant and potentially toxic OPs in complex water matrices.

5. Declaration of Competing Interest

The authors declare no known competing financial interest or personal relationship that could have influence on the work reported in this paper.

6. Acknowledgments

This study was funded by the Deutsche Forschungsgemeinschaft (DFG-German Research Foundation) under the Project Numbers 428639365 (GZ: HU 2699/1-1 and RE 1290/8-1). We would like to thank Danika Ahoor (TUM) for her contributions in solving the gas humidity problems, Dr. Ignacio Sottorff (TUM) for his consistent support and understanding, and Elaine Jennings (UFZ) for feedback and discussion.

7. References

Bader, H. and Hoigné, J. 1981. Determination of ozone in water by the indigo method. Water Research 15(4), 449-456. https://doi.org/10.1016/0043-1354(81)90054-3.

Betsholtz, A., Juárez, R., Svahn, O., Davidsson, Å., Cimbritz, M. and Falås, P. 2022. Ozonation of 14C-labeled micropollutants – mineralization of labeled moieties and adsorption of transformation products to activated carbon. Water Research 221, 118738. https://doi.org/10.1016/j.watres.2022.118738.

547 Borowska, E., Bourgin, M., Hollender, J., Kienle, C., McArdell, C.S. and von Gunten, U. 2016.
548 Oxidation of cetirizine, fexofenadine and hydrochlorothiazide during ozonation: Kinetics and
549 formation of transformation products. Water Research 94, 350-362.
550 https://doi.org/10.1016/j.watres.2016.02.020.
551 Bourgin, M., Beck, B., Boehler, M., Borowska, E., Fleiner, J., Salhi, E., Teichler, R., von
552 Gunten, U., Siegrist, H. and McArdell, C.S. 2018. Evaluation of a full-scale wastewater
553 treatment plant upgraded with ozonation and biological post-treatments: Abatement of
554 micropollutants, formation of transformation products and oxidation by-products. Water
555 Research 129, 486-498. https://doi.org/10.1016/j.watres.2017.10.036.
556 Brunner, A.M., Vughs, D., Siegers, W., Bertelkamp, C., Hofman-Caris, R., Kolkman, A. and ter
557 Laak, T. 2019. Monitoring transformation product formation in the drinking water
558 treatments rapid sand filtration and ozonation. Chemosphere 214, 801-811.
559 https://doi.org/10.1016/j.chemosphere.2018.09.140.
560 Dodd, M.C., Rentsch, D., Singer, H.P., Kohler, H.-P.E. and von Gunten, U. 2010.
561 Transformation of β-Lactam Antibacterial Agents during Aqueous Ozonation: Reaction
562 Pathways and Quantitative Bioassay of Biologically-Active Oxidation Products.
563 Environmental Science & Technology 44(15), 5940-5948.
564 https://doi.org/10.1021/es101061w.
565 Eggen, R.I.L., Hollender, J., Joss, A., Schärer, M. and Stamm, C. 2014. Reducing the
566 Discharge of Micropollutants in the Aquatic Environment: The Benefits of Upgrading
567 Wastewater Treatment Plants. Environmental Science & Technology 48(14), 7683-7689.
568 https://doi.org/10.1021/es500907n.
569 Gao, S., Zhao, Z., Xu, Y., Tian, J., Qi, H., Lin, W. and Cui, F. 2014. Oxidation of
570 sulfamethoxazole (SMX) by chlorine, ozone and permanganate - A comparative study.
571 Journal of Hazardous Materials 274, 258-269.
572 https://doi.org/10.1016/j.jhazmat.2014.04.024.
573 Gómez-Ramos, M.d.M., Mezcua, M., Agüera, A., Fernández-Alba, A.R., Gonzalo, S.,
574 Rodríguez, A. and Rosal, R. 2011. Chemical and toxicological evolution of the antibiotic
575 sulfamethoxazole under ozone treatment in water solution. Journal of Hazardous Materials
576 192(1), 18-25. https://doi.org/10.1016/j.jhazmat.2011.04.072.
577 Gulde, R., Clerc, B., Rutsch, M., Helbing, J., Salhi, E., McArdell, C.S. and von Gunten, U.
578 2021. Oxidation of 51 micropollutants during drinking water ozonation: Formation of
579 transformation products and their fate during biological post-filtration. Water Research 207,
580 117812. https://doi.org/10.1016/j.watres.2021.117812.
581 Huber, M.M., Göbel, A., Joss, A., Hermann, N., Löffler, D., McArdell, C.S., Ried, A., Siegrist,
582 H., Ternes, T.A. and von Gunten, U. 2005. Oxidation of Pharmaceuticals during Ozonation
583 of Municipal Wastewater Effluents: A Pilot Study. Environmental Science & Technology
584 39(11), 4290-4299. https://doi.org/10.1021/es048396s.
585 Huber, M.M., Ternes, T.A. and von Gunten, U. 2004. Removal of Estrogenic Activity and
586 Formation of Oxidation Products during Ozonation of 17α-Ethinylestradiol. Environmental
587 Science & Technology 38(19), 5177-5186. https://doi.org/10.1021/es035205x.
588 Hübner, U., von Gunten, U. and Jekel, M. 2015. Evaluation of the persistence of
589 transformation products from ozonation of trace organic compounds–a critical review. Water
590 Research 68, 150-170. https://doi.org/10.1016/j.watres.2014.09.051.
591 Jennings, E.K., Olea, M.S., Kaesler, J.M., Hübner, U., Reemtsma, T. and Lechtenfeld, O.J.
592 2022. Stable Isotope Labeling for Detection of Ozonation Byproducts in Effluent Organic
593 Matter with FT-ICR-MS. Water Research, 119477.
594 https://doi.org/10.1016/j.watres.2022.119477.
595 Kolkman, A., Martijn, B.J., Vughs, D., Baken, K.A. and van Wezel, A.P. 2015. Tracing
596 Nitrogenous Disinfection Byproducts after Medium Pressure UV Water Treatment by Stable
597 Isotope Labeling and High Resolution Mass Spectrometry. Environmental Science &
598 Technology 49(7), 4458-4465. https://doi.org/10.1021/es506063h.
599 Lee, Y. and Von Gunten, U. 2016. Advances in predicting organic contaminant abatement
600 during ozonation of municipal wastewater effluent: reaction kinetics, transformation
601 products, and changes of biological effects. Environmental Science: Water Research &
602 Technology 2(3), 421-442. https://doi.org/10.1039/C6EW00025H.

603 Lim, S., McArdell, C.S. and von Gunten, U. 2019. Reactions of aliphatic amines with ozone:
604 Kinetics and mechanisms. Water Research 157, 514-528.
605 https://doi.org/10.1016/j.watres.2019.03.089.
606 Lim, S., Shi, J.L., von Gunten, U. and McCurry, D.L. 2022. Ozonation of Organic Compounds
607 in Water and Wastewater: A Critical Review. Water Research, 118053.
608 https://doi.org/10.1016/j.watres.2022.118053.
609 Liu, Z., Craven, C.B., Huang, G., Jiang, P., Wu, D. and Li, X.-F. 2019. Stable Isotopic Labeling
610 and Nontarget Identification of Nanogram/Liter Amino Contaminants in Water. Analytical
611 Chemistry 91(20), 13213-13221. https://doi.org/10.1021/acs.analchem.9b03642.
612 Loos, M., Gerber, C., Corona, F., Hollender, J. and Singer, H. 2015. Accelerated isotope fine
613 structure calculation using pruned transition trees. Analytical Chemistry 87(11), 5738-5744.
614 https://doi.org/10.1021/acs.analchem.5b00941.
615 Loos, R., Carvalho, R., António, D.C., Comero, S., Locoro, G., Tavazzi, S., Paracchini, B.,
616 Ghiani, M., Lettieri, T., Blaha, L., Jarosova, B., Voorspoels, S., Servaes, K., Haglund, P.,
617 Fick, J., Lindberg, R.H., Schwesig, D. and Gawlik, B.M. 2013. EU-wide monitoring survey
618 on emerging polar organic contaminants in wastewater treatment plant effluents. Water
619 Research 47(17), 6475-6487. https://doi.org/10.1016/j.watres.2013.08.024.
620 Mairinger, T. and Hann, S. (2020) Metabolic Flux Analysis in Eukaryotic Cells: Methods and
621 Protocols. Nagrath, D. (ed), pp. 1-16, Springer US, New York, NY.
622 https://doi.org/10.1007/978-1-0716-0159-4_1.
623 Margot, J., Kienle, C., Magnet, A., Weil, M., Rossi, L., de Alencastro, L.F., Abegglen, C.,
624 Thonney, D., Chèvre, N., Schärer, M. and Barry, D.A. 2013. Treatment of micropollutants
625 in municipal wastewater: Ozone or powdered activated carbon? Science of the Total
626 Environment 461-462, 480-498. https://doi.org/10.1016/j.scitotenv.2013.05.034.
627 Mawhinney, D.B., Vanderford, B.J. and Snyder, S.A. 2012. Transformation of 1H-
628 Benzotriazole by Ozone in Aqueous Solution. Environmental Science & Technology 46(13),
629 7102-7111. https://doi.org/10.1021/es300338e.
630 Müller, J., Drewes, J.E. and Hübner, U. 2017. Sequential biofiltration–A novel approach for
631 enhanced biological removal of trace organic chemicals from wastewater treatment plant
632 effluent. Water Research 127, 127-138. https://doi.org/10.1016/j.watres.2017.10.009.
633 Müller, J., Drewes, J.E. and Hübner, U. 2019. Investigating synergies in sequential
634 biofiltration-based hybrid systems for the enhanced removal of trace organic chemicals from
635 wastewater treatment plant effluents. Environmental Science: Water Research &
636 Technology 5(8), 1423-1435. https://doi.org/10.1039/C9EW00181F.
637 Real, F.J., Benitez, F.J., Acero, J.L., Sagasti, J.J.P. and Casas, F. 2009. Kinetics of the
638 Chemical Oxidation of the Pharmaceuticals Primidone, Ketoprofen, and Diatrizoate in
639 Ultrapure and Natural Waters. Industrial & Engineering Chemistry Research 48(7), 3380-
640 3388. https://doi.org/10.1021/ie801762p.
641 Reemtsma, T., Weiss, S., Mueller, J., Petrovic, M., González, S., Barcelo, D., Ventura, F. and
642 Knepper, T.P. 2006. Polar Pollutants Entry into the Water Cycle by Municipal Wastewater:
643 A European Perspective. Environmental Science & Technology 40(17), 5451-5458.
644 https://doi.org/10.1021/es060908a.
645 Spahr, S., Bolotin, J., Schleucher, J., Ehlers, I., von Gunten, U. and Hofstetter, T.B. 2015.
646 Compound-Specific Carbon, Nitrogen, and Hydrogen Isotope Analysis of N-
647 Nitrosodimethylamine in Aqueous Solutions. Analytical Chemistry 87(5), 2916-2924.
648 https://doi.org/10.1021/ac5044169.
649 Spahr, S., von Gunten, U. and Hofstetter, T.B. 2017. Carbon, Hydrogen, and Nitrogen Isotope
650 Fractionation Trends in N-Nitrosodimethylamine Reflect the Formation Pathway during
651 Chloramination of Tertiary Amines. Environmental Science & Technology 51(22), 13170-
652 13179. https://doi.org/10.1021/acs.est.7b03919.
653 Tekle-Röttering, A., von Sonntag, C., Reisz, E., Eyser, C.v., Lutze, H.V., Türk, J., Naumov, S.,
654 Schmidt, W. and Schmidt, T.C. 2016. Ozonation of anilines: Kinetics, stoichiometry,
655 product identification and elucidation of pathways. Water Research 98, 147-159.
656 https://doi.org/10.1016/j.watres.2016.04.001.
657 Tentscher, P.R., Lee, M. and von Gunten, U. 2019. Micropollutant Oxidation Studied by
658 Quantum Chemical Computations: Methodology and Applications to Thermodynamics,

659 Kinetics, and Reaction Mechanisms. Accounts of Chemical Research 52(3), 605-614.
660 https://doi.org/10.1021/acs.accounts.8b00610.
661 Ternes, T.A., Stüber, J., Herrmann, N., McDowell, D., Ried, A., Kampmann, M. and Teiser, B.
662 2003. Ozonation: a tool for removal of pharmaceuticals, contrast media and musk
663 fragrances from wastewater? Water Research 37(8), 1976-1982.
664 https://doi.org/10.1016/S0043-1354(02)00570-5.
665 Valkenborg, D., Mertens, I., Lemière, F., Witters, E. and Burzykowski, T. 2012. The isotopic
666 distribution conundrum. Mass Spectrometry Reviews 31(1), 96-109.
667 https://doi.org/10.1002/mas.20339.
668 von Gunten, U. 2003. Ozonation of drinking water: Part I. Oxidation kinetics and product
669 formation. Water Research 37(7), 1443-1467. https://doi.org/10.1016/S0043-
670 1354(02)00457-8.
671 von Gunten, U. 2018. Oxidation Processes in Water Treatment: Are We on Track?
672 Environmental Science & Technology 52(9), 5062-5075.
673 https://doi.org/10.1021/acs.est.8b00586.
674 Von Sonntag, C. and Von Gunten, U. (2012) Chemistry of ozone in water and wastewater
675 treatment, IWA publishing. https://doi.org/10.2166/9781780400839.Wert, E.C., Rosario-
676 Ortiz, F.L., Drury, D.D. and Snyder, S.A. 2007. Formation of oxidation byproducts from
677 ozonation of wastewater. Water Research 41(7), 1481-1490.
678 https://doi.org/10.1016/j.watres.2007.01.020.
679 Willach, S., Lutze, H.V., Eckey, K., Löppenberg, K., Lüling, M., Terhalle, J., Wolbert, J.-B.,
680 Jochmann, M.A., Karst, U. and Schmidt, T.C. 2017. Degradation of sulfamethoxazole
681 using ozone and chlorine dioxide - Compound-specific stable isotope analysis,
682 transformation product analysis and mechanistic aspects. Water Research 122, 280-289.
683 https://doi.org/10.1016/j.watres.2017.06.001.
684 Yu, H., Ge, P., Chen, J., Xie, H. and Luo, Y. 2017. The degradation mechanism of
685 sulfamethoxazole under ozonation: a DFT study. Environmental Science: Processes &
686 Impacts 19(3), 379-387. https://doi.org/10.1039/C6EM00698A.
687 Zucker, I., Mamane, H., Riani, A., Gozlan, I. and Avisar, D. 2018. Formation and degradation
688 of N-oxide venlafaxine during ozonation and biological post-treatment. Science of the Total
689 Environment 619, 578-586. https://doi.org/10.1016/j.scitotenv.2017.11.133.

690